

CFD Simulation of Fibrous Debris Blockage for a 4 Loop Westinghouse Plant

Yiban Xu¹, Jin Yan¹, Peng Yuan¹,
Robert A. Brewster², Zeses Karoutas¹

¹Westinghouse Electric Company, Cranberry Township, PA, USA

²CD-adapco, Melville, NY, USA

xuy@westinghouse.com

INTRODUCTION

Multi-physics virtual reactor models have been developed under sponsorship of DOE's Consortium for Advanced Simulation of Light Water Reactors (CASL) project [1]. In order to demonstrate some of CASL's simulation capabilities on a high-performance computing system, the Advanced Modeling and Applications (AMA) team piloted a full core simulation of a 4 loop Westinghouse NSSS with postulated fibrous debris accumulation at the core inlet following a LOCA event.

Fibrous debris may be formed in the current fleet of nuclear power reactors during the blowdown phase in a Loss Of Coolant Accident (LOCA). Subsequently, the debris could be entrained in the recirculated cooling flow and could block narrow flow paths in the core, such as bottom nozzles, fuel assembly grids, etc. Reduced core flow due to debris blockage may cause over-heating and even boiling.

The paper presents development of a Computational Fluid Dynamics (CFD) model of a Westinghouse Four Loop PWR with STAR-CCM+ [2] to simulate the aforementioned issue. The CFD results give the details of flow and void fraction (when boiling occurs) fields, as well as temperature fields in the coolant and the solid structures (pellet, cladding, grids, bottom and top nozzles) in the core under complicated transient accident conditions. Due to the large model size and computing resource requirements, this endeavor also provides valuable experiences in identifying CFD model development issues (labor, time and code limitations) and in challenging the capacity of computing resources.

This CFD model simulates the pressure drop increase across the bottom nozzle region with time, postulated as the fibrous debris gradually accumulated in the region. With careful consideration of plant accident conditions, i.e., asymmetric flow configuration, decay heat variations in time and in space, Conjugate Heat Transfer (CHT) between the solids and the coolant, and phase change due to possible boiling, it is hoped that the CFD model will provide insights into the fluid flow and temperature distribution under such complex situations.

DESCRIPTION OF THE CFD MODELING

The CFD model consists of 360° of the reactor vessel, including the cold and the hot legs. The geometries of the reactor internals were meshed in great detail, except for the spacer grids, which were represented by porous media. The mesh of the reactor core was built in PROSTAR [3]; while the meshes of the remaining regions of the reactor vessel were built using the STAR-CCM+ polyhedral mesher. The various meshes were assembled into a single domain connected through interfaces on the Westinghouse large-memory-sharing workstation, counting total of more than 1.2 billion cells. Physical models (including VOF-based boiling) were applied with appropriate boundary and initial conditions.

The fibrous debris blockage process simulation is assumed to start in a transient mode at 18 minutes after a hot leg LOCA (assuming the reactor to be in a recirculation cooling mode at this moment, i.e. RHR injection flows only). The pressure drop in the bottom nozzle region was ramped up (assuming fibrous debris uniformly accumulated) at 2 s after the transient simulation started. The ramp-up was completed in 30 s. The simulation was continued for 1 minute after the ramp was completed. Heating power is implemented in the fuel pellets using a power density table obtained from the ANC neutronics code calculations. The core power table is first multiplied by the decay power curve and then interpolated on the calculation nodes.

The simulation was executed on Westinghouse computer clusters and the INL Fission computer. Total of about 94 s physical time was completed in the 55 hrs/CPU. Post-processing was done on the Westinghouse large-memory-sharing workstation. Figure 1 shows the arrangement of inlets and outlet of the CFD model.

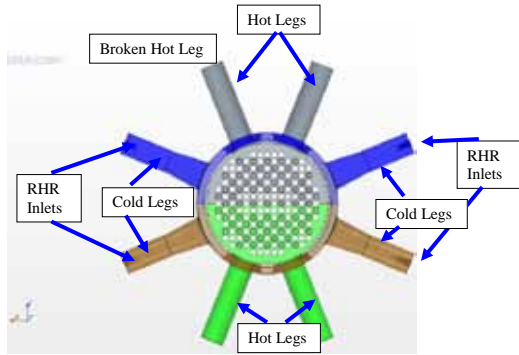


Figure 1 Hot Legs, Cold Legs and RHR Inlets

RESULTS

Pressure Drops Across Bottom Nozzle and Core

Area averaged total pressure differences across the bottom nozzle region and the entire core are depicted in Figure 2. The ramp up of pressure drop became visible at about 5 s and a different slope appeared from 10 s, indicating the beginning of the second segment of the imposed pressure drop ramp. After an additional 20 s (i.e., at ~25 s), the second ramp slope completes and the pressure drop ramp becomes constant. Boiling starts at about 20 s. The pressure drop across the bottom nozzle region jumps higher due to void generation in the core. A negative pressure drop was observed in the core region after boiling starts. Note that the total pressure is the static pressure obtained by isentropically bringing the flow to rest, excluding hydrostatic component. Therefore, the negative pressure drop in the core was the result of that the coolant in the upper core region flows faster due to higher void fraction, producing higher total pressure. The pressure drop in the bottom nozzle region was stabilized after 30 s; while the pressure drop in the core region continued to increase negatively due to void fraction generation.

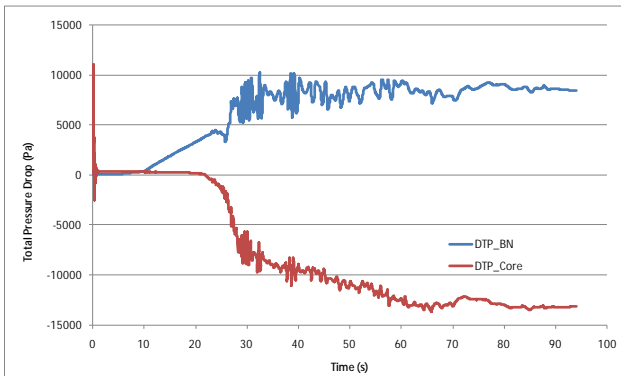


Figure 2 Total pressure drops across bottom nozzle and core

Vapour Accumulation and Flow at Broken Leg

After boiling started, it is interesting to see how vapor was accumulated and exited the broken hot leg. Figure 3 depicts the vapor mass accumulation in the whole computational domain and the time variation of the vapor mass flow rate at the broken hot. It is clear that the vapor mass accumulation became noticeable at about 20 s; however, the vapor flow through the exit occurred after 40 s, indicating the vapor transfer time from the core to the exit. Both vapor generation rate and exit flow rate were slightly decreased after about 80 s, but both were still increasing. More simulation time may be needed in order to reach equilibrium.

Figure 4 shows the volume fraction of vapor at the horizontal cut plane through the outlet nozzle center line. This void fraction profile reflects the lateral flow toward the broken hot leg. The closer to the broken hot leg, the higher the void fraction occurs. There is some liquid remaining in the guide tube assemblies at this moment. The liquid seems continue to deplete as seen in the contour plot of the vertical cut plane in Figure 5. The liquid in the guide tubes seems to be depleted slowly in this simulation. This could be caused by certain approximations in the top boundary to reduce computing cost, the vessel upper head was not included. Instead, a solid wall boundary was applied at the boundary of the guide tube assemblies. Vapor appears in the upper region of the core, indicating the coolant experiences boiling in this region.

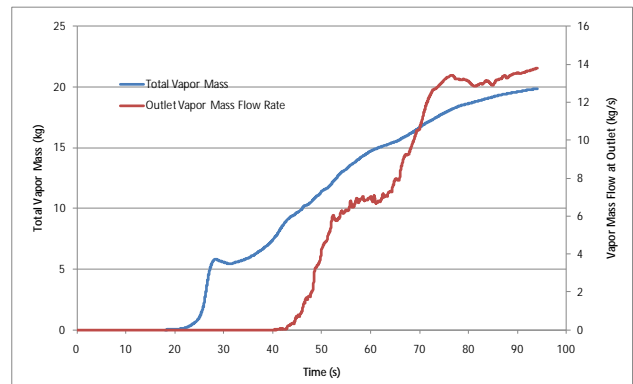


Figure 3 Vapor Accumulation and Vapor Flow At Exit

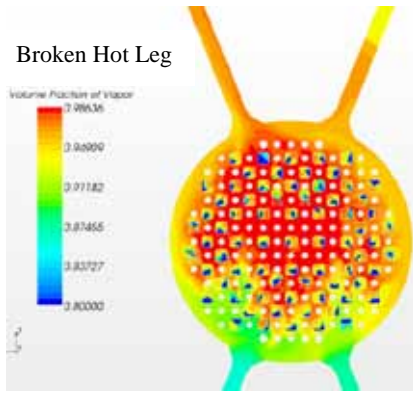


Figure 4 Void Fraction Profile at Horizontal Plane of Outlet Nozzle Center Line

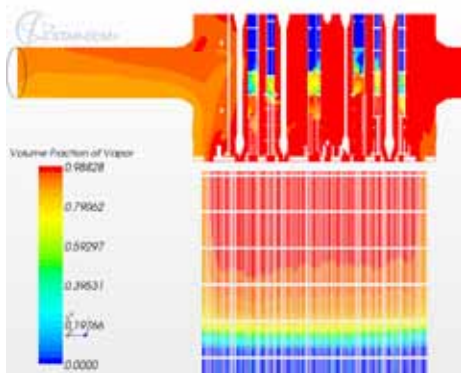


Figure 5 Void Distribution in Vertical Plane through Broken Hot Leg

Vector Plot of Bypass and Core Inlet Flows

The vector plot near the core inlet in Figure 6 shows the evidence of downward flow in the bypass channel at this moment. The high speed jets (only one is shown) through the holes on the former plates produced strong circulating flow zones in the bypass channel. This downward flow may be created by the high pressure losses in the upper plenum and the exit nozzle regions, which pushes the coolant into the bypass channel through the opening holes at the top of the core shroud.

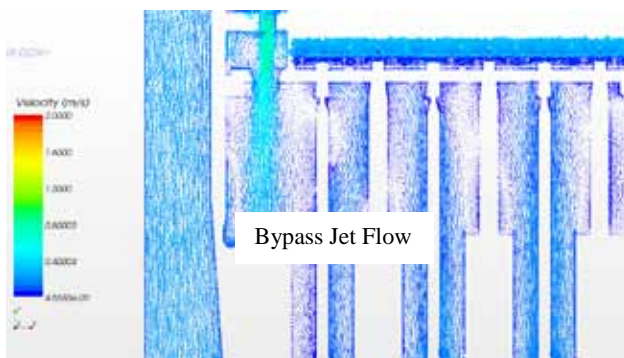


Figure 6 Velocity of Bypass Flow near Core Inlet

Maximum Temperatures in Pellets and Cladding Outer Surfaces

Maximum temperatures in pellets and on outside surfaces of claddings are ultimately interested in terms of fuel operating safety. This model had monitored these variables all the time during the run over all computational cells and the results are shown in Figure 7. These temperatures increase rapidly in the first 15 s due to decay power heating and limited heat transfer from single phase flow. Once the surface temperature reaches saturation temperature and boiling starts, temperature increase rate slows down. Pellet center line experiences boiling heat transfer a few second later (visible at about 20 s). Since cladding outer surface temperature tracks the coolant temperature, superheated vapor appears in the coolant region. This may be one of limitations of the VOF boiling model since it assumes that the liquid and vapor have the same temperature and interfacial heat transfer factor was predetermined. It needs to point out that longer simulation time may be necessary if the peak temperatures are desired to appear.

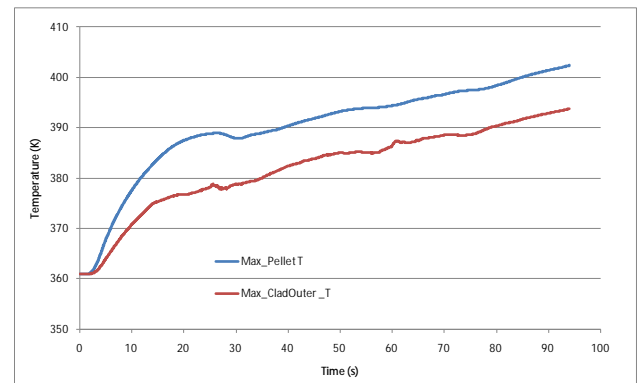


Figure 7 Maximum Temperatures in Pellet and Cladding Outer Surface Regions

CONCLUSIONS

It is technically challenging to accurately simulate flow and heat transfer in large and complex systems, such as whole reactor vessels -- the difficulty coming from multiple aspects, including, but not limited to, complicated physics, complex geometry, and difficult meshing. Nevertheless, CFD predictions can provide insights of flow and thermal phenomena which may not be easily obtained from other approaches. The current model has represented the following major processes related to the fibrous debris blockage issue that has been modeled:

- Pressure drop ramp-up due to fibrous debris accumulation in the bottom nozzle region
- Decay heat variation in both time and in space

- Boiling model implementation based on VOF framework
- Complete reactor vessel geometry
- Asymmetric accident configuration

The results of the CFD simulation provide fluid flow, void fraction and temperature distributions in the reactor vessel. Noticeably, bypass channel may experience downward flow during the transient; the water inside the guide tubes in the upper plenum region may need a long time to become fully depleted.

Overall, the CFD approach is far more timely, economical, safe, and environmentally friendly than any other options, such as testing in plants or predictions using system codes, with respect to the generated insights obtained. Actual plant testing is expensive and time consuming, while system codes can only model the reactor core in limited numbers of channels [4]. This exercise shows that modeling of this type problem is quite practical, cost-effective and uniquely capable. The experience gained in this process provides guidelines of future advancement in personnel preparation, network connection, computing software and hardware configuration or combination of both.

Important conclusions consist of a few recommendations for future efforts. Thorough validation of boiling model is recommended; Eulerian boiling is preferred. Two-phase flow modeling sensitivity analysis may be conducted with smaller sub-models.

The future development of modeling fibrous debris blockage for water reactors is listed below:

- Continue to run this model until peak temperature appears
- Investigate the influence of the upper head region
- Implement the Eulerian Multi-Phase Flow model, including boiling
- Implement a detailed Fibrous Debris Transport simulation if available
- Implement more realistic initial conditions, such as thermal energy distributions in the coolant and solids
- Benchmarking efforts may be necessary to improve porous medium model accuracy and determine if the spacer grids should be explicitly modeled.
- Simplify core modeling of pellets, claddings and grids to run the model faster.

The last, but not the least, high fidelity of the developed CFD model also makes other applications possible, such as thermal mixing and boric acid precipitation in the reactor lower plenum and the core during normal operations, participated transients and/or under accidental conditions.

ACKNOWLEDGEMENTS

The authors gratefully acknowledge the support of the staff of the Idaho National Laboratory High Performance Computing Center, with special thanks to Dr. Tamara Grimmett.

REFERENCES

1. Yan, J. et al., Multi-Physics Computational Models Development for Westinghouse PWRs, to be submitted to ANS 2013 Winter Meeting, November 2013, Washington DC.
2. CD-adapco STAR-CCM+ 7.04.006 User's Guide, www.cd-adapco.com
3. CD-adapco PROSTAR User's Guide, www.cd-adapco.com
4. pbadupws.nrc.gov/docs/ML1129/ML11292A021.pdf WCAP-16793-NP, "Evaluation of Long-Term Cooling Considering Particulate, Fibrous and Chemical Debris in the Recirculating Fluid", October, 2011